UNIVERSIDADE D COIMBRA

FACULDADE DE CIÊNCIAS E TECNOLOGIA

Study on the influence of the yield surface shape in the hole expansion test

Marta C. Oliveira[1] • Diogo M. Neto[1] • José L. Alves[2] • Luís F. Menezes[1]

[1] University of Coimbra, CEMMPRE, Department of Mechanical Engineering, Portugal

[2] University of Minho, CMEMS, Department of Mechanical Engineering, Portugal

iddrg 2020 VIRTUAL-KOREA

26-30 October 2020
South Korea

Hole expansion test

- Edge cracking occurring during the stretch-flanging process of AHSS cannot be accurately predicted by the FLD
- The AHSS edge cracking resistance is commonly evaluated:
  - Using a sheet specimen that contains a central hole and the tools are axisymmetric
  - The hole expansion ratio (hole edge crack) defines the edge cracking resistance

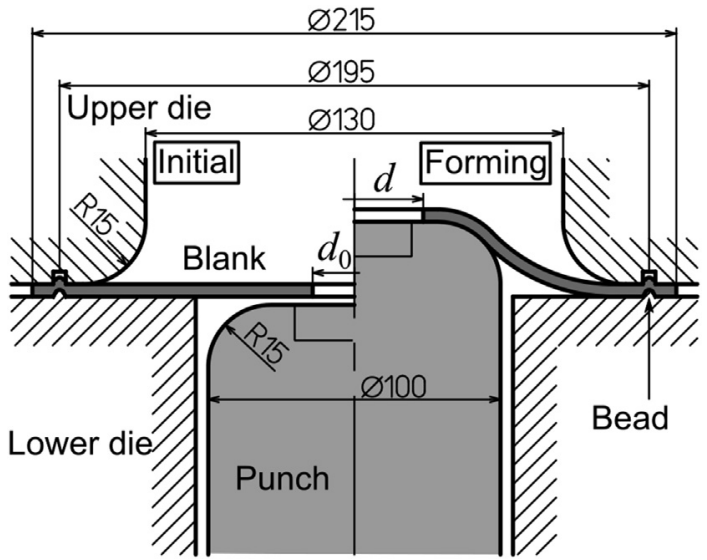

Cylindrical punch

Fractured specimen

M.C. Oliveira (marta.oliveira@dem.uc.pt)

Hole expansion test

Benchmark 1 (Numisheet 2018): Hole expansion of a high strength steel sheet

- Dual Phase steel (DP980) sheet with 1.2 mm of thickness
- Central hole with 30 mm of diameter
- Periphery of the blank is clamped using a draw-bead (force about 800 kN)

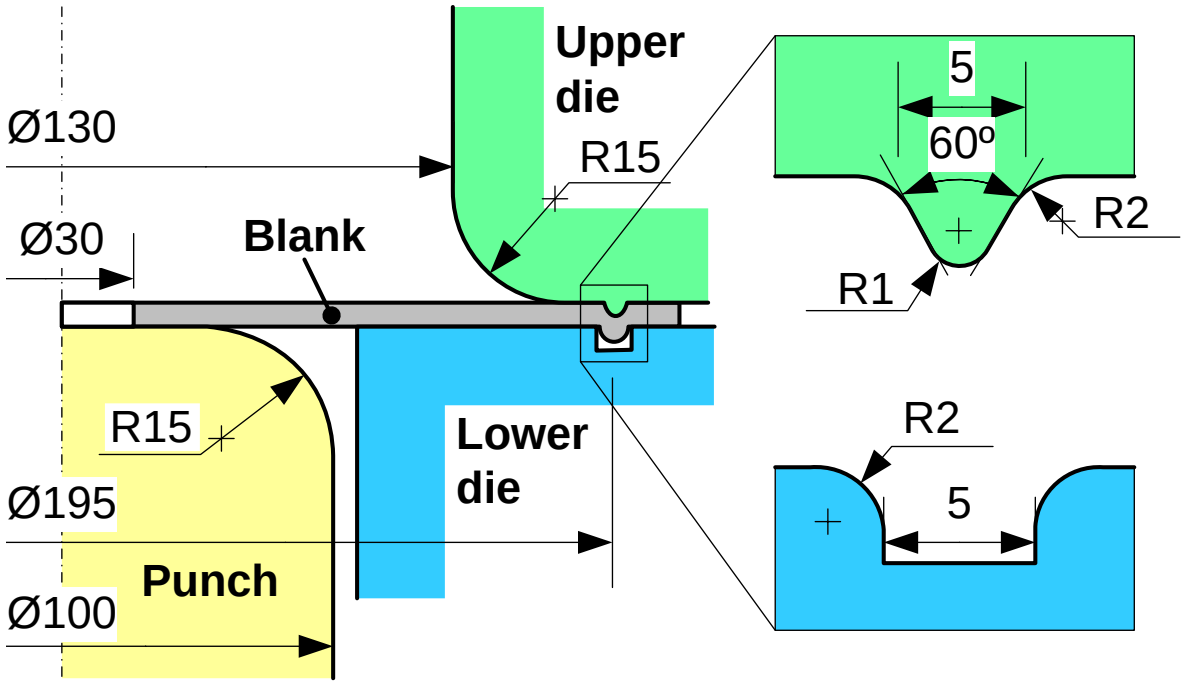

Geometry of the forming tools and specimen used in the hole expansion test

M.C. Oliveira (marta.oliveira@dem.uc.pt)

Hole expansion test

Finite element model

- DD3IMP in-house finite element code (implicit time integration)
- 1/4 of the model (symmetry conditions)
- Forming tools are assumed rigid discretized by Nagata patches
- Blank discretized by linear hexahedral (8-nodes) finite elements

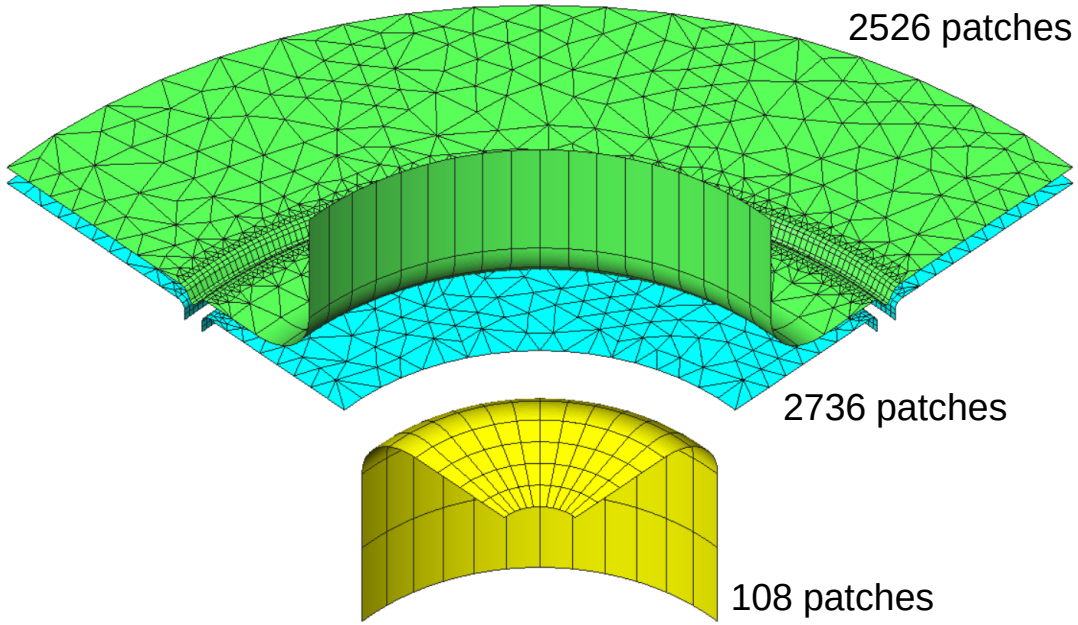

64,800 finite elements

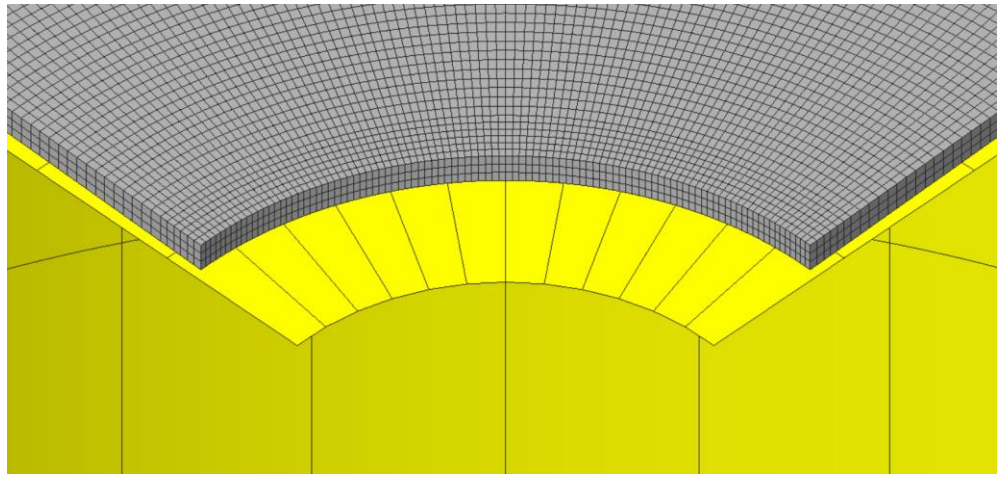

3 layers of finite elements in the thickness direction

100 finite elements in the circumferential direction

M.C. Oliveira (marta.oliveira@dem.uc.pt)

Finite element model

- The Coulomb friction law is adopted:
  - Lubricated punch−blank interface: inclusion of a layer of Teflon (0.3 mm thick) between the blank and the punch head (μ=0.0)
  - No lubricant on the interfaces between the blank and the upper/lower dies (μ=0.15)
- Plastic behavior of the specimen modelled by the Swift law (isotropic work hardening) combined with an associated flow rule and the CPB06ex2 yield criterion.

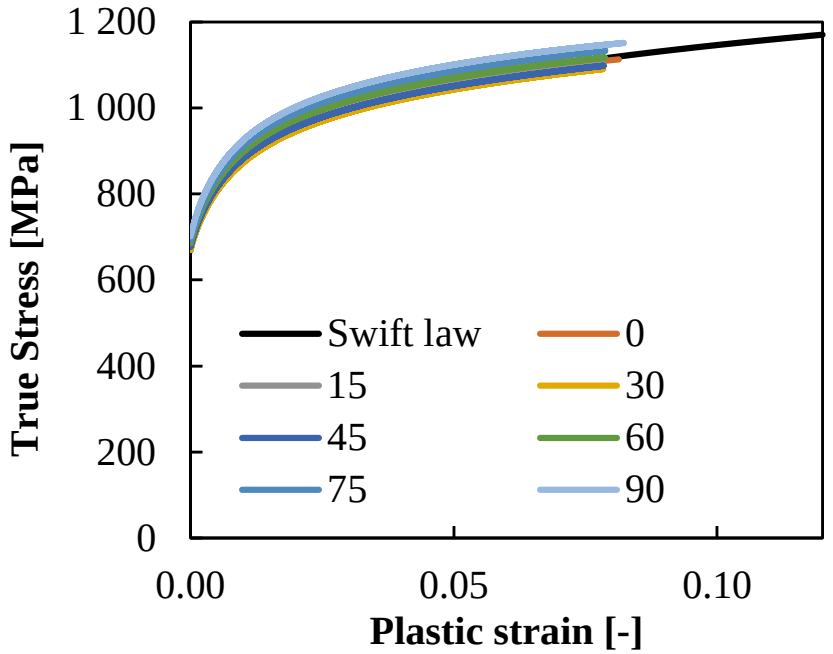

True stress *versus* equivalent plastic strain curve

M.C. Oliveira (marta.oliveira@dem.uc.pt)

Yield criterion

Cazacu, Plunkett and Barlat, 2006 (CPB06)

$$Y = B\left[\left(|s_1| - k\,s_1\right)^a + \left(|s_2| - k\,s_2\right)^a + \left(|s_3| - k\,s_3\right)^a\right]^{\frac{1}{a}}$$

where $\mathbf{s} = \mathbf{C}\boldsymbol{\sigma}'$

$$\mathbf{C} = \begin{bmatrix} C_{11} & C_{12} & C_{13} & 0 & 0 & 0 \\ C_{12} & C_{22} & C_{23} & 0 & 0 & 0 \\ C_{13} & C_{23} & C_{33} & 0 & 0 & 0 \\ 0 & 0 & 0 & C_{44} & 0 & 0 \\ 0 & 0 & 0 & 0 & C_{55} & 0 \\ 0 & 0 & 0 & 0 & 0 & C_{66} \end{bmatrix}$$

Anisotropy parameters

$C_{11}, C_{22}, C_{33}, C_{66}, C_{12}, C_{13}, C_{23}$

$$B = \left[\frac{1}{\left(|\phi_1| - k\,\phi_1\right)^a + \left(|\phi_2| - k\,\phi_2\right)^a + \left(|\phi_3| - k\,\phi_3\right)^a}\right]^{\frac{1}{a}}$$

$$\begin{Bmatrix} \phi_1 \\ \phi_2 \\ \phi_3 \end{Bmatrix} = \begin{Bmatrix} (2/3)C_{11} - (1/3)C_{12} - (1/3)C_{13} \\ (2/3)C_{21} - (1/3)C_{22} - (1/3)C_{23} \\ (2/3)C_{31} - (1/3)C_{32} - (1/3)C_{33} \end{Bmatrix}$$

Asymmetry parameter

k

- **Two linear transformations** - Plunkett, Cazacu and Barlat, 2008 (CPB06ex2): where $\mathbf{s}' = \mathbf{C}'\boldsymbol{\sigma}'$
  - Due to the homogeneity in stresses of the yield function it is recommended to set C_{11}=1.0. Therefore, for 3-D stress conditions this orthotropic yield criterion involves 17 anisotropy coefficients

M.C. Oliveira (marta.oliveira@dem.uc.pt)

DD3MAT: objective function

$$F(\mathbf{A}) = w_{\sigma_\theta} \sum_\theta \left(\sigma_\theta(\mathbf{A}, \bar{\varepsilon}^p) / \sigma_\theta(\bar{\varepsilon}^p) - 1 \right)^2 + w_{r_\theta} \sum_\theta \left(r_\theta(\mathbf{A}) / r_\theta - 1 \right)^2$$

$$+ w_{\beta_\varphi} \sum_\varphi \left(\beta_\varphi(\mathbf{A}, \bar{\varepsilon}^p) / \beta_\varphi(\bar{\varepsilon}^p) - 1 \right)^2$$

$\mathbf{A}$ – set of anisotropy parameters

σ_θ – yield stresses in uniaxial tension

r_θ – anisotropy coefficients in uniaxial tension

β_φ – direction of plastic strain rate in biaxial tension

θ – angle from the rolling direction

φ – loading direction

w_i – weighting coefficients

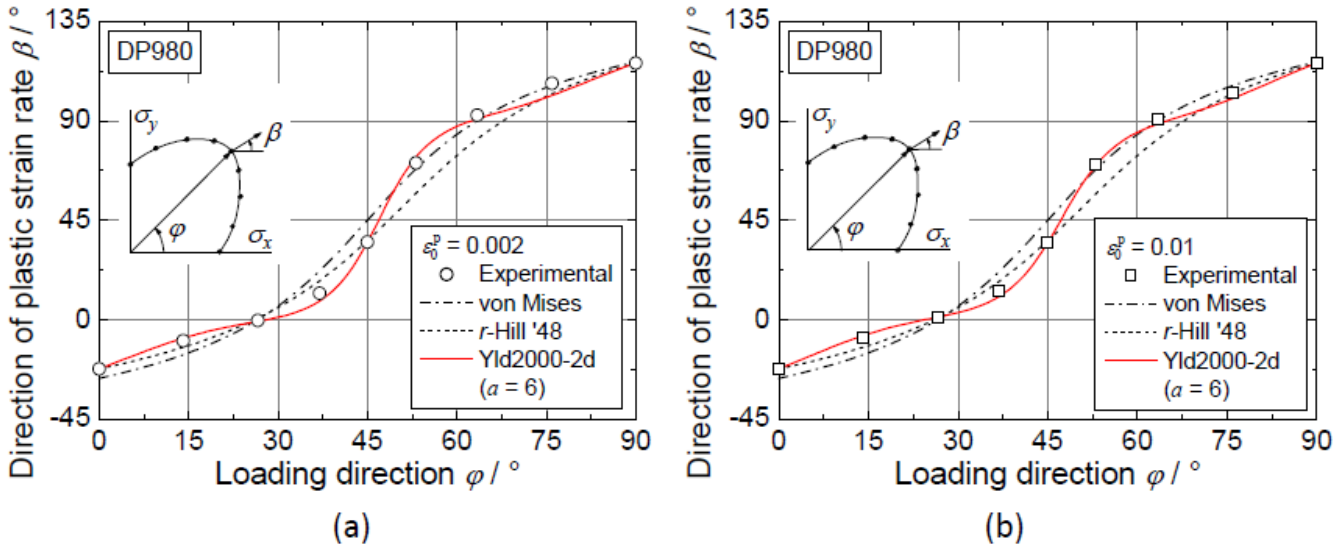

Directions of the plastic strain rates measured at (a) ε^p_0=0.002 and (b) ε^p_0=0.01, compared with those calculated using the von Mises, Hill '48, and the Yld2000-2d yield functions [Kuwabara *et al.* 20018, *Benchmark 1 – Hole expansion of High Strength Steel Sheet, Part A: Benchmark Description*].

- Minimized with a downhill simplex method

M.C. Oliveira (marta.oliveira@dem.uc.pt)

Identification of the anisotropy parameters

- Based on the *r*-value and yield stress in-plane directionalities and on the β values (ε^p_0=0.01). Since there is no experimental data for compression stress states, *k*=*k*'=0.0
- This procedure was performed considering **different even integer values** for the homogeneity parameter a, trying to assure a similar description of the trends of the experimental values, which required the use of different sets of weighting coefficients. For example:

a = 2

c_{11}	c_{22}	c_{33}	c_{66}	c_{23}	c_{13}	c_{12}	Others
1.0000	0.6340	-1.0307	1.0012	-0.0003	0.1467	0.0004	1.0000

c'_{11}	c'_{22}	c'_{33}	c'_{66}	c'_{23}	c'_{13}	c'_{12}	Others
0.9981	-0.9892	1.0001	1.0116	0.0238	0.0000	0.0000	1.0000

a = 6

c_{11}	c_{22}	c_{33}	c_{66}	c_{23}	c_{13}	c_{12}	Others
1.0000	1.1413	1.0072	-1.2103	0.0101	-0.4768	0.0328	1.0000

c'_{11}	c'_{22}	c'_{33}	c'_{66}	c'_{23}	c'_{13}	c'_{12}	Others
1.1748	0.6263	1.1548	1.3050	-0.3582	0.3499	-0.3300	1.0000

M.C. Oliveira (marta.oliveira@dem.uc.pt)

DP980 orthotropic behaviour

Identification of the anisotropy parameters

- For the *r*-values, the maximum error occurs for the two lower values of a, at RD, attaining a maximum value of ~11% for a =4
- For the normalized yield stresses, the maximum error also occurs for the two lower values of a, with a =2 overestimating the yield stress for TD (~9%) while for a = 4 this value is underestimated by ~3%.

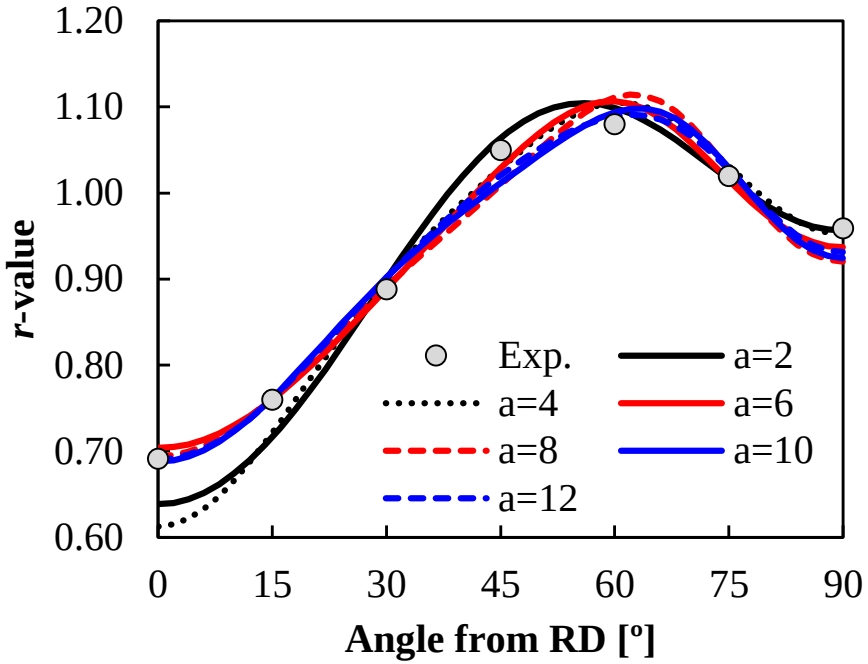

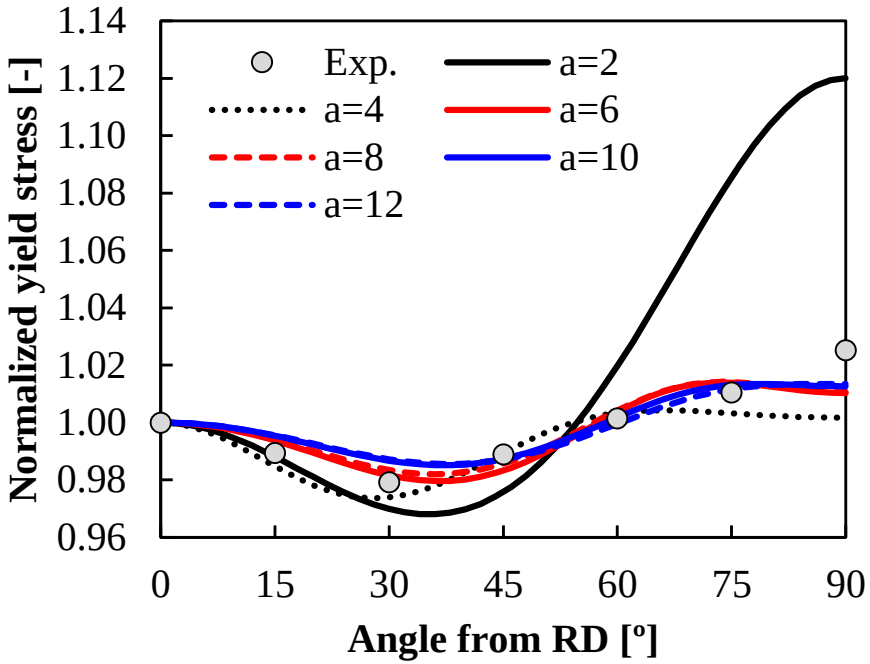

M.C. Oliveira (marta.oliveira@dem.uc.pt)

Identification of the anisotropy parameters

- For the directions of the plastic strain rate, the maximum error also occurs for the two lower values of a, with a=2 showing a particular different trend between the equibiaxial tension and plane strain along TD (maximum error of ~23%). For a =4, the maximum error reduces to ~12%

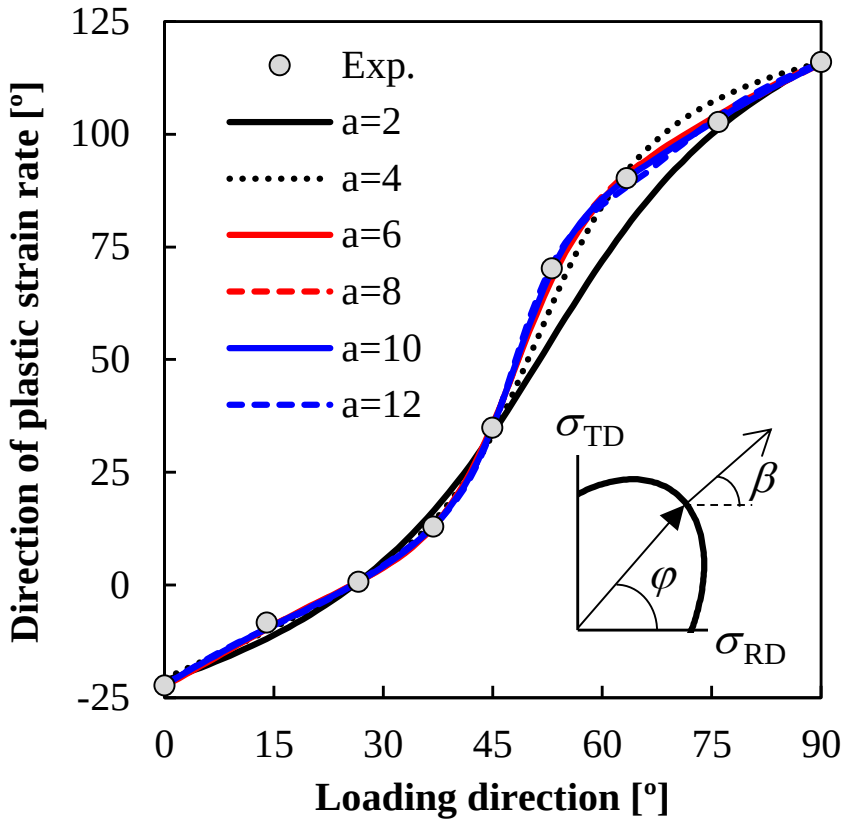

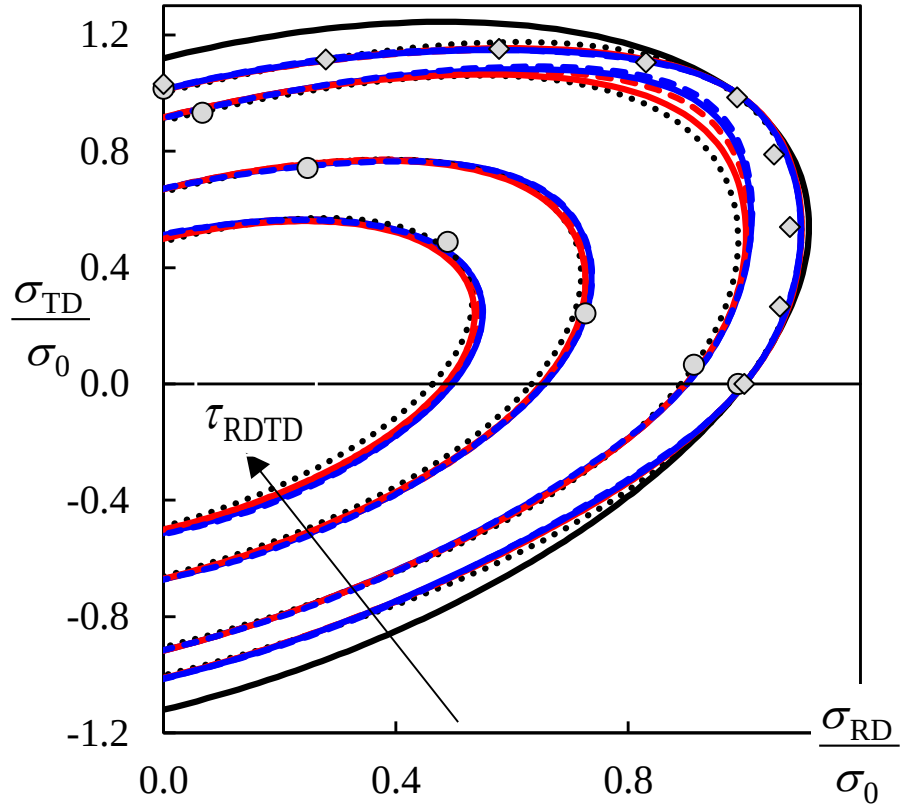

Analysis of the Stress state

- Consider a specimen with a central hole submitted to an uniform displacement in the outer edge
- One quarter is considered to enable the analysis of the behavior using the von Mises yield criterion

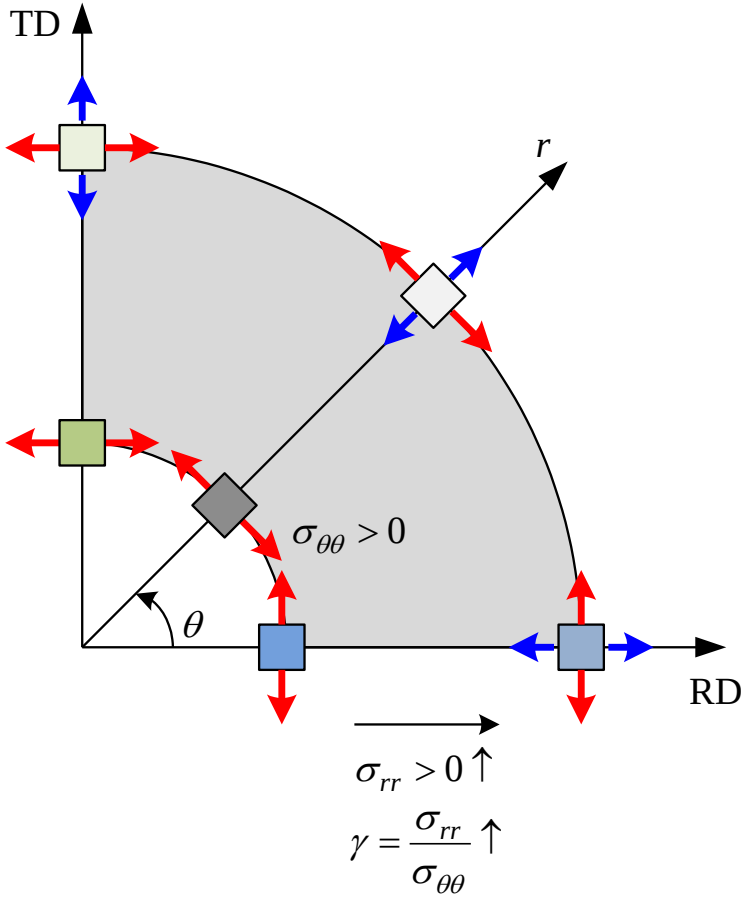

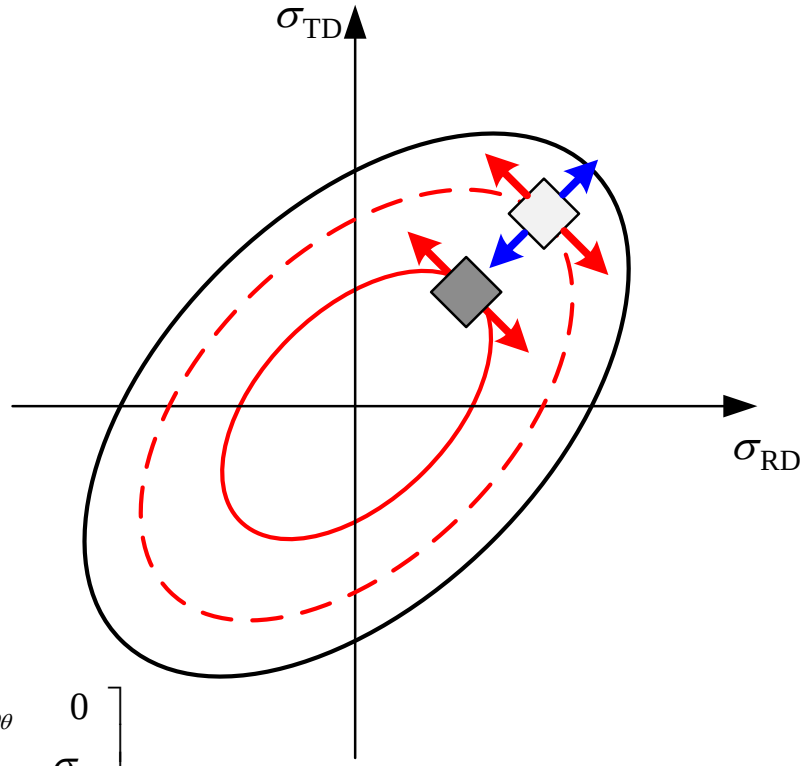

$$\boldsymbol{\sigma} = \begin{bmatrix} \sigma_{rr} & 0 \\ 0 & \sigma_{\theta\theta} \end{bmatrix} = \begin{bmatrix} \gamma\sigma_{\theta\theta} & 0 \\ 0 & \sigma_{\theta\theta} \end{bmatrix}$$

$$\hat{\boldsymbol{\sigma}} = \mathbf{R}\boldsymbol{\sigma}\mathbf{R}^{\mathrm{T}} = \begin{bmatrix} \cos\theta & \sin\theta \\ -\sin\theta & \cos\theta \end{bmatrix} \begin{bmatrix} \sigma_{rr} & 0 \\ 0 & \sigma_{\theta\theta} \end{bmatrix} \begin{bmatrix} \cos\theta & -\sin\theta \\ \sin\theta & \cos\theta \end{bmatrix} = \begin{bmatrix} \sigma_{RD} & \tau_{RTD} \\ \tau_{RTD} & \sigma_{TD} \end{bmatrix}$$

M.C. Oliveira (marta.oliveira@dem.uc.pt)

Hole expansion: Simple test

Analysis of the Stress state

- Assuming that the ratio between the radial and the circumferential stress can attain a maximum of 1.0, the stress states for the material points located at an angle θ to RD cover the first quadrant of the yield loci (von Mises material)

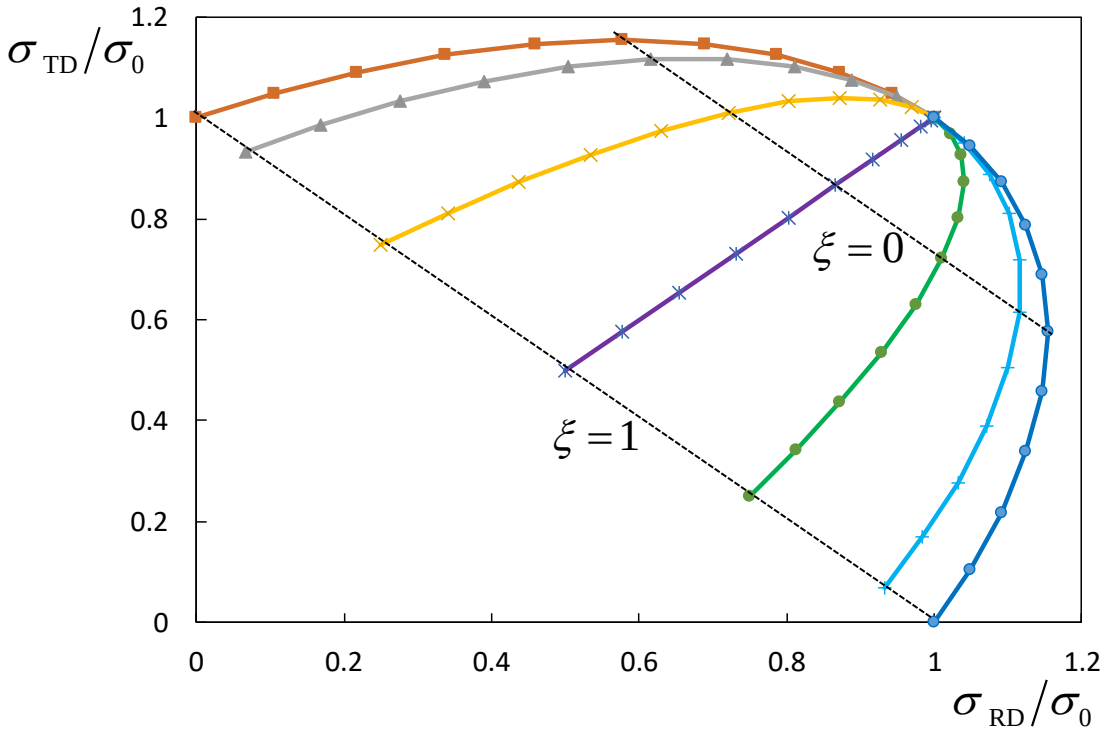

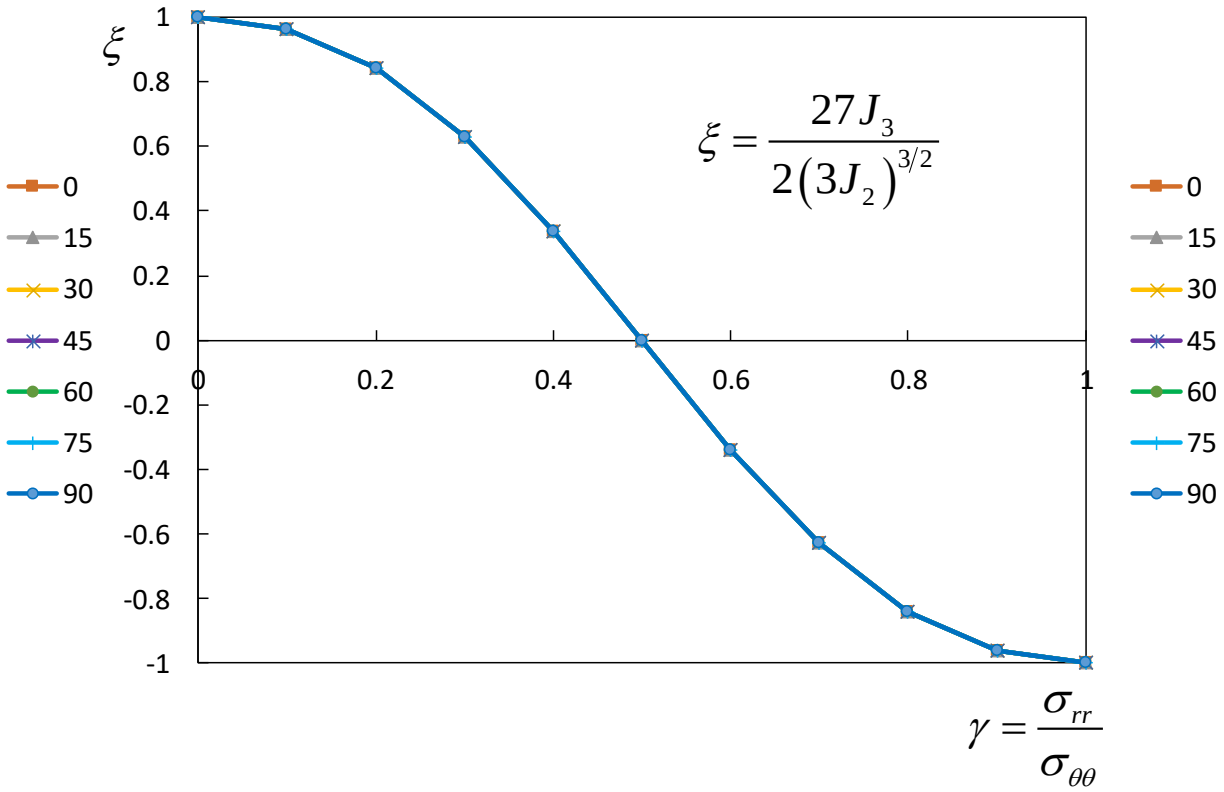

Hole expansion test: DP980

Numerical simulation results

- The onset of necking was experimentally predicted for a stroke of 20 mm along the RD, at a distance from the hole edge of about 7.5 mm, which is similar to the one observed for the sets of parameters with $a \geq 6$

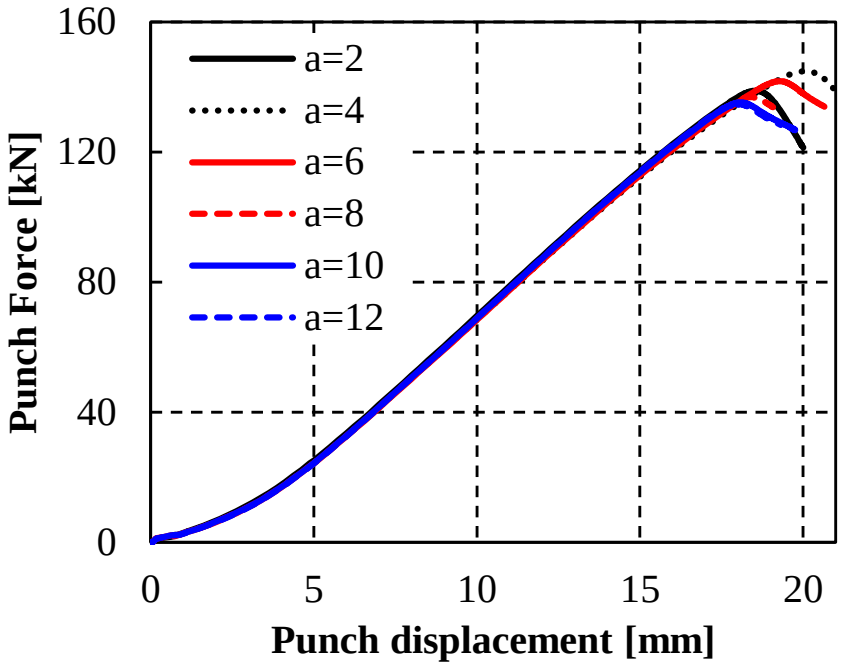

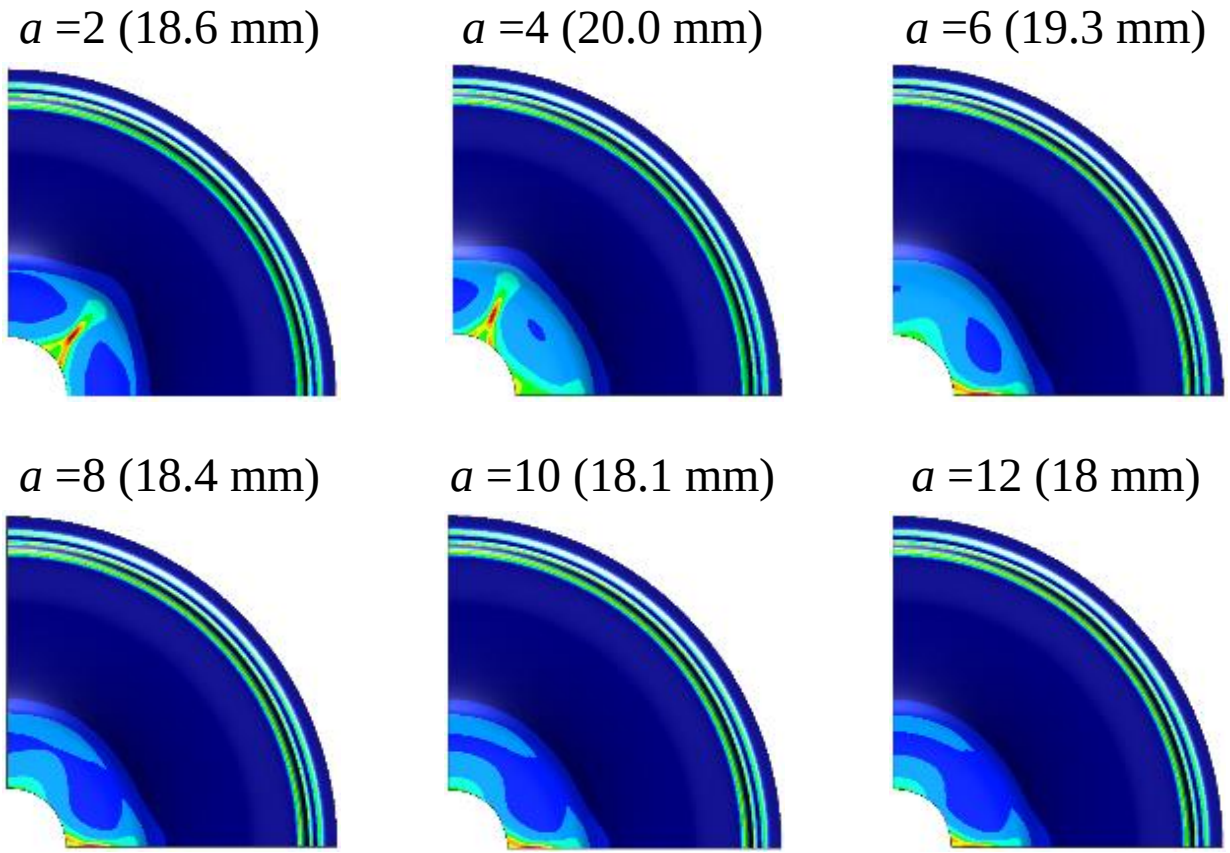

M.C. Oliveira (marta.oliveira@dem.uc.pt)

Hole expansion test: DP980

Numerical simulation results (stroke of 15 mm)

- The experimental results predict the highest decrease in thickness along the TD, followed by the RD and DD
- The numerical results predict the lowest decrease in thickness along the DD while the RD presents the highest, except for a =2. For increasing values of a, the thickness strain along RD and TD tends to become more negative, while for the DD the trend is opposite

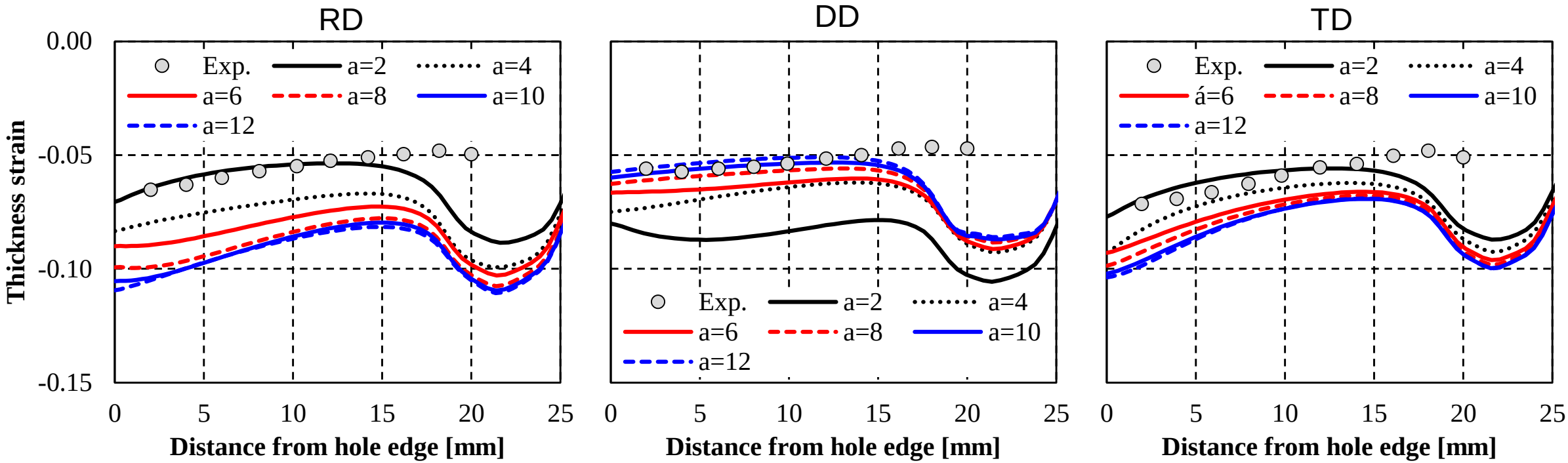

M.C. Oliveira (marta.oliveira@dem.uc.pt)

Hole expansion test: DP980

Numerical simulation results (stroke of 15 mm)

- Although the trend for the distribution at 2 mm from the hole edge is globally well predicted (except for a =2), the variation is overestimated. This seems to be related with the trend predicted for the radial displacement at 2 mm from the hole edge
- Taking into account the similarities observed between the yield surfaces for both RD and TD, particularly for $a \geq 6$, this indicates that the compatibility with the surrounding material also affects the strain distributions

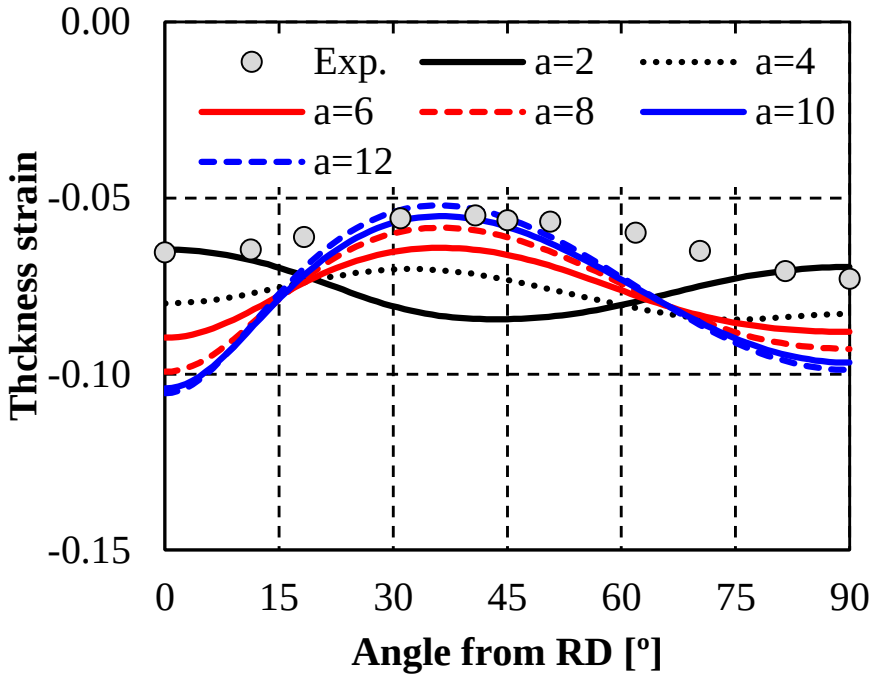

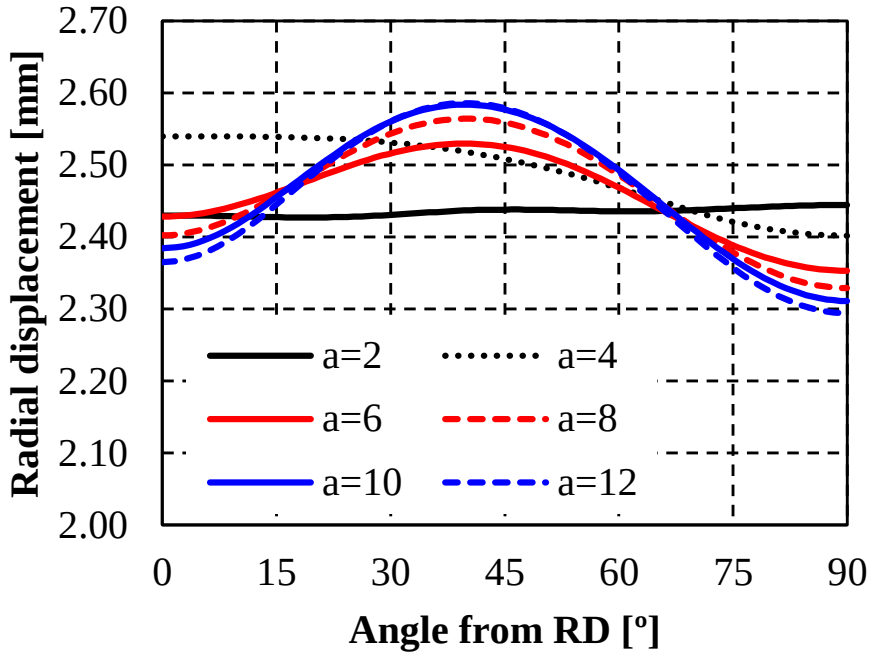

Hole expansion test: DP980

Numerical simulation results (stroke of 15 mm)

- The ratio between the radial and the circumferential stress components presents slight differences for each radial direction and evolves during the forming process. Since the Lode parameter attains the null value for a ratio of 0.5, the plane strain state is not located in the immediate surrounding to the hole edge

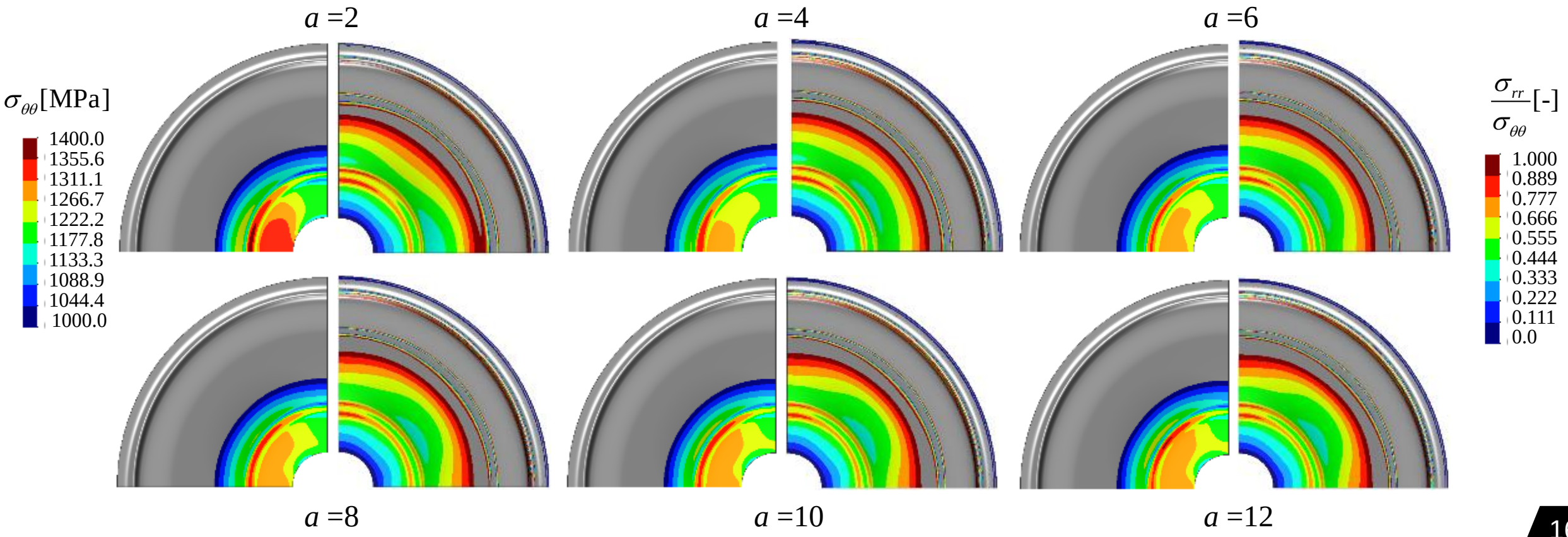

M.C. Oliveira (marta.oliveira@dem.uc.pt)

Hole expansion test: DP980

Numerical simulation results (a = 6)

- The evolution of the stress state for points located at the same initial distance from the hole follows a similar trend, for the different orientations to RD

$$\xi \uparrow \Rightarrow \gamma = \frac{\sigma_{rr}}{\sigma_{\theta\theta}} \downarrow$$

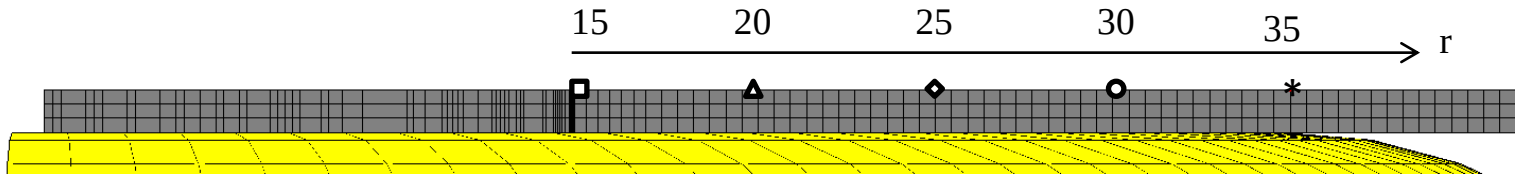

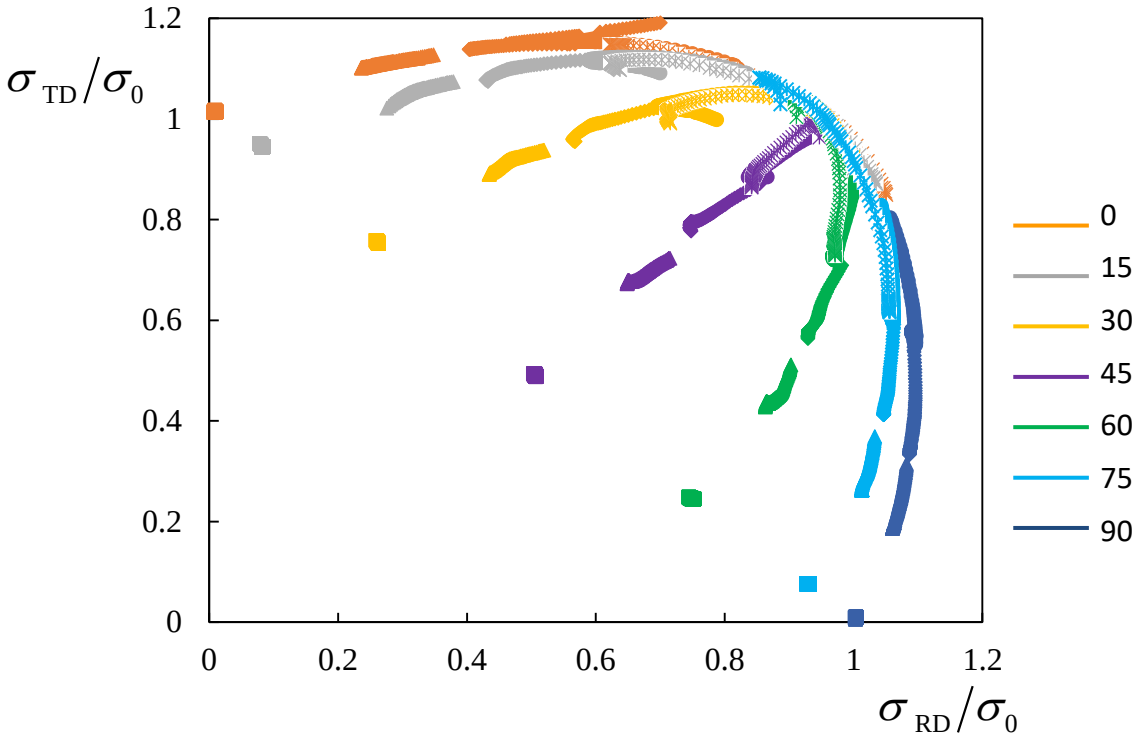

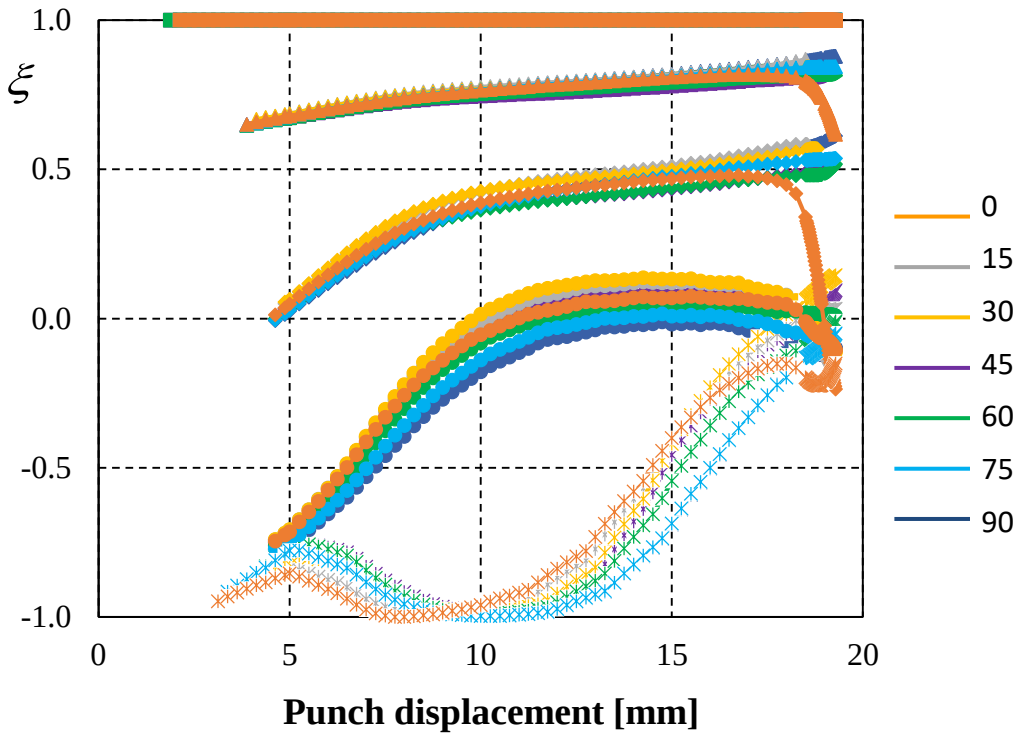

Hole expansion test: DP980

Numerical simulation results (a = 6)

- The analysis of the selected points, located along RD, indicates that the strain localization seems to occur first for points located at an initial distance from the middle between 20 and 25 mm. Once the strain localization occurs this points tend to a plane strain state

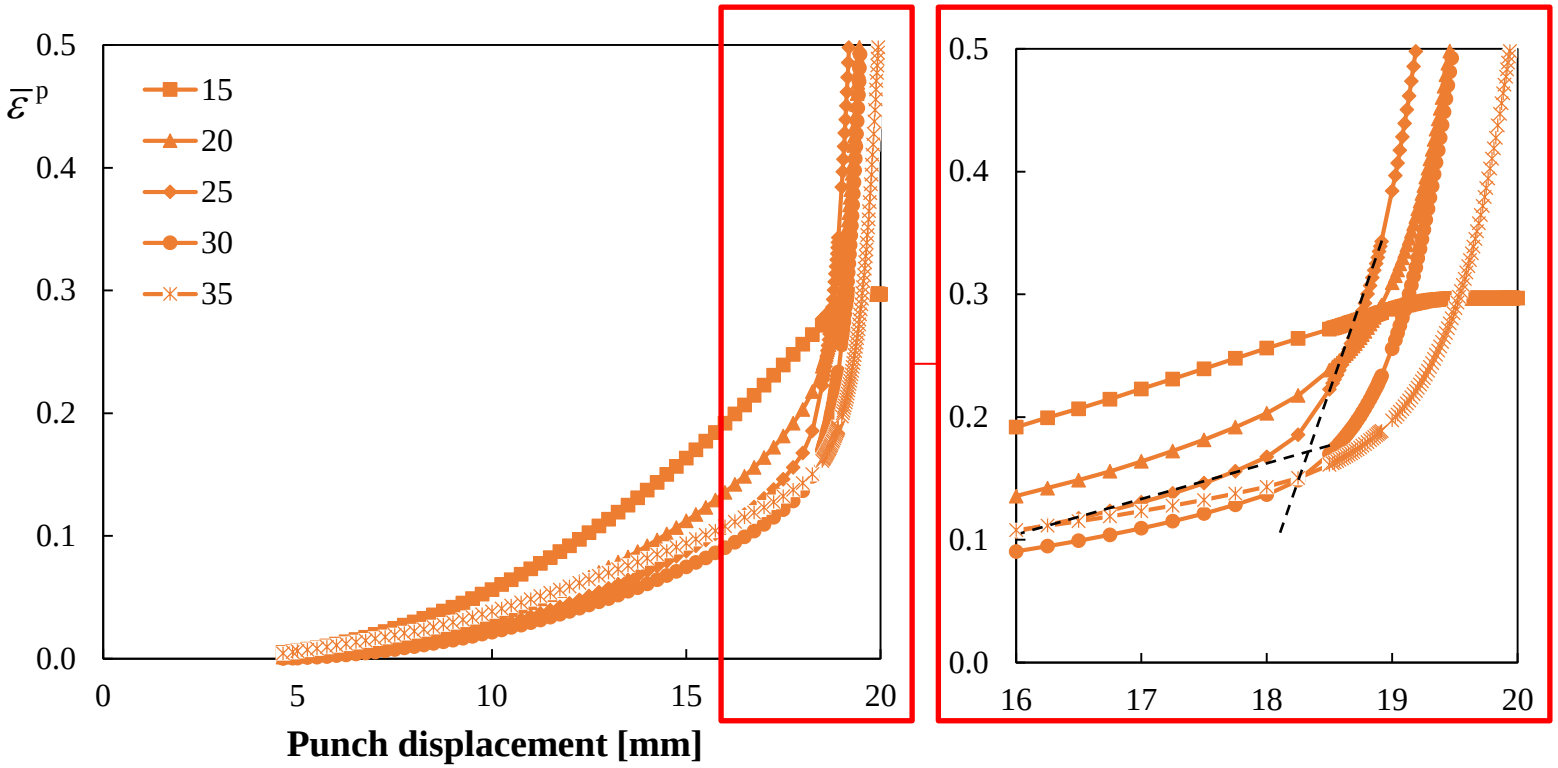

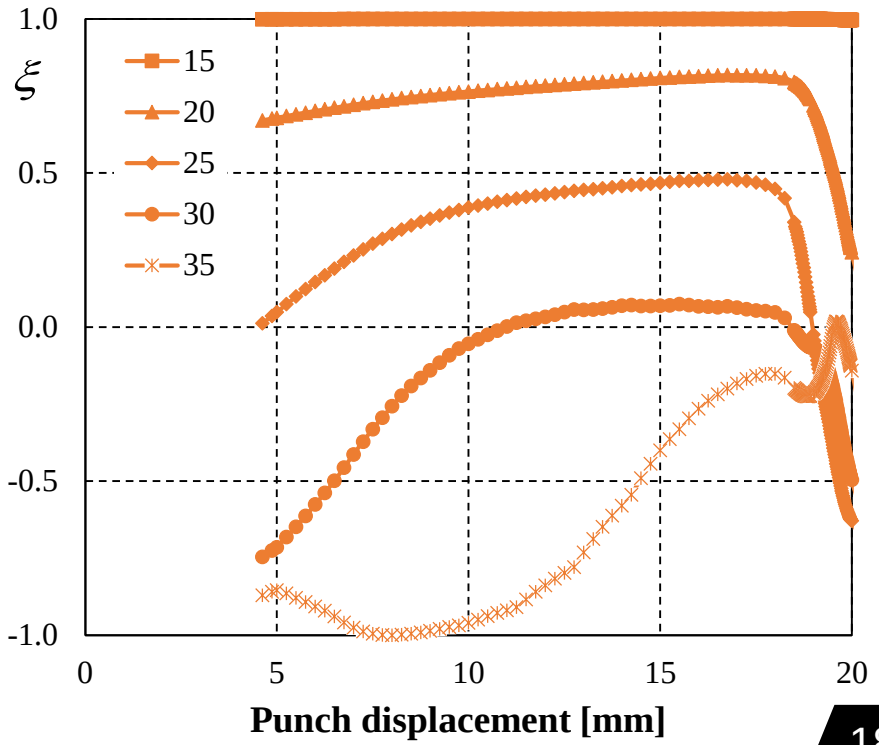

Conclusions

- The analysis of the hole expansion test indicates that the flat zone **is submitted to stress states from uniaxial tension** at the hole free edge (circumferential direction), **to balanced biaxial tension** between the radial and the circumferential directions, close to the punch radius.

- The rotation of these stress tensors to the material frame, defined by the principal axis of anisotropy, shows that the flat zone of the hole expansion tests covers a **wide range of stress states** located in the tension-tension quadrant of the yield surface in the RD-TD plane, considering also different in-plane shear stress components.

- The accurate prediction of the strain distributions and, consequently, the onset of necking requires an accurate description of the **yield surface shape** for all this range, when adopting an associated flow rule.

- Although this may imply performing a wider range of experimental test (e.g. biaxial tension of cruciform specimens cut in different directions to RD), it may contribute to improve the prediction of defects.

M.C. Oliveira (marta.oliveira@dem.uc.pt)

Acknowledgements

The authors gratefully acknowledge the financial support of the **Portuguese Foundation for Science and Technology** (FCT) under projects with reference PTDC/EME-EME/30592/2017 and PTDC/EME-EME/31657/2017 and by European Regional Development Fund (ERDF) through the Portugal 2020 program and the Centro 2020 Regional Operational Programme (CENTRO-01-0145-FEDER-031657) under the project MATIS (CENTRO-01-0145-FEDER-000014) and UIDB/00285/2020.

Projetos Cofinanciados pela UE:

FCT Fundação para a Ciência e a Tecnologia

CENTRO 2020

PORTUGAL 2020

UNIÃO EUROPEIA
Fundo Europeu de Desenvolvimento Regional